Bio-based substances from urban waste as auxiliaries for solar photo-Fenton treatment under mild conditions: Optimization of operational variables

(Article begins on next page)

19 October 2024

Bio-based substances from urban waste as auxiliaries for solar photo-Fenton treatment under mild conditions: optimization of operational variables

J. Gomis[1], L. Carlos[2], A. Bianco Prevot[3], A. C. S. C. Teixeira[4], M. Mora[5], A.M. Amat[1], R. Vicente[1], A. Arques[1*].

(1) Grupo de Procesos de Oxidación Avanzada, Dpto de Ingeniería Textil y Papelera, Universitat Politècnica de València. Plaza Ferrándiz y Carbonell s/n, Alcoy, Spain. aarques@txp.upv.es.

(2) Instituto de Investigaciones Fisicoquímicas Teóricas y Aplicadas (INIFTA), CCT-La Plata-CONICET, Universidad Nacional de La Plata, Diag 113 y 64, La Plata, Argentina.

(3) Dipartimento di Chimica, Università di Torino, Via Giuria 7, Torino, Italy.

(4) Escola Politécnica da Universidade de São Paulo, Av. Prof. Luciano Gualberto, tr.3, 380, São Paulo, Brasil.

(5) Dpto de Matemática Aplicada, Universitat Politècnica de València. Plaza Ferrándiz y Carbonell s/n, Alcoy, Spain.

*Corresponding author: aarques@txp.upv.es, phone: ++34 966528417

Abstract

The use of soluble bio-based organic substances (SBO) obtained from urban wastes to expand the pH region where the photo-Fenton process can be applied has been

22 investigated in this study. For this purpose, a mixture of six pollutants, namely

23 acetaminophen, carbamazepine, amoxicillin, acetemiprid, clofibric acid and caffeine, at

24 an initial concentration of 5 mg L^{-1} each, has been employed. Surface response

25 methodology, based on the Doehlert matrix, has shown to be a useful tool to determine

26 the effect of pH (in the range 3-7), concentration of SBO (15-25 mg L^{-1}) and iron (2-6

27 mg L^{-1}) on the performance of the photodegradation of the studied pollutants, measured

28 by their half-life. Results indicate that, at high SBO concentration, the optimum pH

29 shifts in most cases to a higher value (between 3 and 4) and that a significant loss of

30 efficiency of the process was only observed at pH values above 5. An iron concentration

31 of 4-5 mg L^{-1} and an amount of SBO of 19-22 mg L^{-1} have been determined to be the

32 optimal conditions for the degradation of most of the studied pollutants at pH = 5.

33

34 **Graphical abstract**
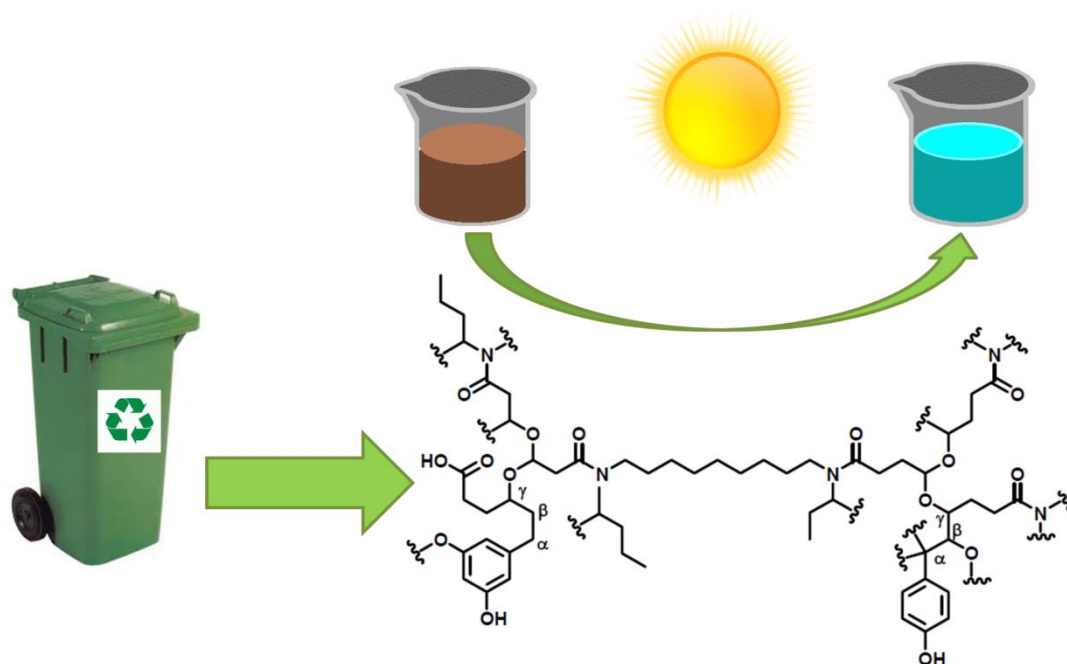
35

36

1. Introduction

Wastes have deserved attention from researchers, as they could be a sustainable source of materials with a wide range of potential applications [1]. In particular, soluble bio-based organic substances (SBO) have been isolated from solid organic wastes submitted to aging under aerobic fermentation conditions, following a process that involves extraction of the soluble fraction at basic pH and posterior precipitation at acidic media [2]. SBO are constituted by a mixture of macromolecules, which average molecular weight ranges from 67 to 463 kg mol^{-1}; they consist of long aliphatic chains, aromatic rings and several oxygen and nitrogen-containing functional groups [2]. Hence, these materials show basic structural similarities with some macromolecules found in natural organic matter (NOM), such as humic and fulvic acids, which play an important role in

3

photochemical processes leading to the self-remediation of ecosystems [3]. In this context, determining the potential use of SBO for water detoxification is meaningful, as this may be considered a green process since it valorises solid wastes as sources of photoactive materials with similar properties as less available NOM. Information on this issue is very scarce, and only some recent papers have been published reporting on the ability of these compounds to act as photocatalysts in the degradation of chlorophenols [4, 5], sulphonic acids [6], dyes [7, 8] or pharmaceuticals [9]. SBOs action can be related to an enhanced photogeneration of reactive species; however, the strong screen effect produced by these coloured materials negatively affects the degradation of pollutants that can undergo direct photolysis. When simulated sunlight was employed as irradiation source, the screen effect becomes predominating, thus making SBOs unattractive as solar photocatalysts [9].

Alternatively, SBOs might also be employed as complexing agents to drive photo-Fenton processes at mild conditions. Photo-Fenton is based on the ability of iron salts to catalyse decomposition of hydrogen peroxide into highly oxidizing species (mainly hydroxyl radicals, although other species might also contribute) in a process that is accelerated by irradiation [10]. One major drawback of this process is the highly acid media required to avoid formation of non-active iron oxides or hydroxides. However, some efforts have been recently made for the implementation of photo-Fenton at circumneutral pH. This approach might be especially useful to treat emerging pollutants (EPs) as a certain loss of efficiency in the generation of reactive species might be acceptable in this case, as EPs are commonly found at low concentration, and hence lesser amounts of oxidizing species are necessary [11, 12]. This strategy can be improved by using chemical auxiliaries, able to form photoactive complexes, at mild

84   pH, with the iron added [13]. Humic acids are among the materials employed for this

85   purpose, because of their ability for iron complexation [13-16].

86

87   Because of their similarity with humic substances, SBOs are also candidates to extend

88   the application of photo-Fenton to pH conditions where iron ions are normally not

89   soluble. Indeed, photo-Fenton process in the presence of SBOs have been recently

90   shown to be able to remove a mixture of EPs at pH=5.2 [9]. Hence, a logical step

91   beyond is to determine the role of the operational parameters on the efficiency of the

92   process. For this purpose, a response surface methodology based on Doehlert design has

93   been chosen in this work in order to determine the effect of SBOs and iron

94   concentrations at the pH interval between 3, close to the optimal value, and 7. The

95   Doehlert design has been commonly employed as a chemometric tool, enabling to

96   minimize the number of experiments required to obtain the surface [17, 18]. The

97   mixture of EPs employed in previous work [9, 16] has been chosen as target solution:

98   acetaminophen, carbamazepine, amoxicillin, acetamiprid, clofibric acid and caffeine

99   (see Figure 1 for structures).

100

101   **2. Experimental**

102   2.1 Reagents

103   Acetaminophen, caffeine, amoxicillin, clofibric acid, carbamazepine and acetamiprid

104   were purchased from Sigma-Aldrich and used as received. Hydrogen peroxide (30%

105   v/v), ferric chloride, sulphuric acid and sodium hydroxide, were obtained from Panreac.

106   Water was Milli-Q grade.

107

108   The SBO employed in this work, namely CVT230, was obtained from urban biowastes

109   supplied by ACEA Pinerolese waste treatment plant (Pinerolo, Italy) following a

110   procedure detailed elsewhere [19]. Briefly, the starting material was compost from

111   gardening-park trimming residues matured for 230 days: it was digested 4 h at 60 °C at

112   alkaline conditions (pH = 13) and 4 V/w water/solid ratio to favour hydrolysis of

113   organics. Alkaline hydrolyzed solution have been recognized as very similar to the

114   humic matter, in turn characterized by the presence of a dimensionally smaller fraction

115   (fulvic acid) soluble in all the pH range, and of a bigger one (humic acid), not soluble

116   below pH 3. Instead of separating the two fraction by means of pH variation, the size

117   difference was exploited. The recovered liquid phase was therefore circulated through a

118   polysulfone ultrafiltration membrane with 5 kD molecular weight cut-off to yield a

119   retentate with 5-10 % dry matter content. The membrane retentate was dried at 60 °C to

120   yield the final water soluble bio-based product (SBO). It contained 72.1% (w/w) of

121   volatile solids and the carbon content was 38.3 % (see [8] for further details).

122

123   2.2 Reactions

124   Experiments were performed in a 250 mL cylindrical Pyrex vessel irradiated with a

125   solar simulator (Sun 2000, ABET Technologies) equipped with a 550 W Xenon Short

126   Arc Lamp. A pyrex glass filter was used to cut off radiation below 300 nm (which only

127   accounted for a residual fraction of the lamp irradiance). The vessel was loaded with an

128   aqueous solution containing the six EPs at an initial concentration of 5 mg L^{-1} each.

129   SBO concentration was varied in the range 15-25 mg L^{-1}; $FeCl_3$ was added to reach a

130   concentration of iron between 2 and 6 mg L^{-1}. The initial amount of hydrogen peroxide

131   was 2.2 mmol L^{-1} in all cases, which is half the stoichiometric amount required to

132   mineralize the EPs; this concentration was employed in order to obtain a relatively slow

133   kinetics, which allows a better determination and comparison of illumination times

134   required to remove the EPs under the different conditions that have been studied. The

135   pH was adjusted to the desired value (3-7) by dropwise addition of either 0.1 mmol L^{-1}

136   NaOH or 0.1 mmol L^{-1} H_2SO_4. Temperature was kept in the range 30-35 ºC throughout

137   the reaction. Samples were periodically taken from the solution, filtered through a

138   polypropylene membrane (0.45μm) and diluted 1:1 with methanol.

139

140   Control experiments showed that direct photolysis of the pollutants was negligible

141   under the employed conditions and irradiation in the presence of H_2O_2 solely resulted in

142   a moderate degradation of amoxicillin (less than 20% after 200 min of irradiation).

143

144   2.3. Analysis

145   The concentration of each EP was determined by UPLC (Perkin Elmer model Flexar

146   UPLC FX-10). A Brownlee Analytical column (DB-C18) was employed as stationary

147   phase. The eluent consisted in a mixture of acetonitrile (A) and a 0.1% formic acid

148   aqueous solution (B); the relative amount of each solvent was changed following a

149   linear gradient, from 3% A to 70% A in 8 min; the flow rate was 0.3 mL min^{-1}.

150   Detection wavelengths were 205 nm (acetaminophen, amoxicillin, caffeine and

151   carbamazepine), 225 nm (clofibric acid) and 245 nm (acetamiprid). Identification and

152   quantification of the EPs were performed by comparison with standards.

153

154   2.4 Surface response methodology

155

156   In order to gain further insight into the effect of the studied operational variables (pH,

157   SBO and iron concentration), an experimental design methodology based on a Doehlert

158   array [20]. In this case, a total of 15 experiments (k^2+k+1, where k is the number of

159   analysed variables, 3 in this study, plus two replicates of the central point) were

160   performed. Experimental conditions of all experiments are found in Table 1. The

161   software Statgraphics Centurion XVI was used for response surface model fitting by

162   means of the least squares method. The illumination time required to degrade each

163   pollutant to 50% of its initial concentration ($t_{50\%}$) was used as response; it was obtained

164   from the plot of the relative EP concentration vs. illumination time.

165

166   **3. Results and discussion**

167

168   Plots of the relative concentration of each EP vs illumination time were obtained for

169   each experiment (see Figure 2 for an example). Considering an illumination time of 90

170   minutes, the results show complete removal of all EPs for the experiments carried out at

171   pH 3. At pH 5, removals between 90 and 100% were obtained for all EPs except

172   acetamiprid, for which removals in the range 54-68.5% were obtained. These results

173   confirm the efficiency of the photo-Fenton reaction under acidic and mildly acidic

174   conditions, the later favoured by the presence of SBOs. Finally, maximum percent

175   removals between 5.7 and 64.7% were obtained for the experiments carried out at pH 7,

176   again the lowest removals after 90 minutes of illumination (5.7-21%) corresponding to

177   acetamiprid. These trends show that the choice of a response like the illumination time

178　necessary to obtain pollutant removals of 90% or greater could not be considered for all

179　EPs and pH for the conditions used in the present study (pollutants initial

180　concentrations, H_2O_2 and iron concentrations) and in some cases would require too long

181　illumination times to be observed.

182

183　As a result, the illumination time required for the removal of 50% of each pollutant

184　($t_{50\%}$) was considered for every experiment (Table 1). From the practical point of view,

185　the response $t_{50\%}$ is not submitted to phenomena such as lack of hydrogen peroxide or

186　changes in the experimental conditions that can affect the kinetic behaviour and/or

187　reproducibility (mainly under the less efficient conditions, where too long illumination

188　times would be required. Based on the response values in Table 1, six three-dimensional

189　full quadratic response surface models were obtained, one for each EP (see Table 2,

190　Equations I-A to I-F). For all EPs the values of the determination coefficient (R^2) were

191　high (92.4; 97.4; 98.1; 97.1; 95.9; and 99.4% for amoxicillin, carbamazepine,

192　acetamiprid, clofibric acid, caffeine, and acetaminophen, respectively), indicating good

193　agreement between experimental and calculated values of the response variable. In each

194　case, the values of the residuals (differences between calculated and measured values of

195　$t_{50\%}$) as a function of measured values were randomly distributed with error zero with

196　zero mean.

197

198　The corresponding ANOVA tables (see Supplementary Data, Tables T1-T6) and the

199　Pareto charts (Figure 3) show that except for acetaminophen, the only significant effect

200　on $t_{50\%}$ at 95% confidence level (p-values < 0.05) was due to pH, as expected, being the

201　reaction faster at lower pH values; the quadratic effect of this variable was significant,

202   indicating the important curvature of the response surfaces. For acetaminophen, the

203   quadratic effect of SBO concentration was also significant. Therefore, simplified model

204   equations for $t_{50\%}$ were fitted by considering the effect of pH only, as presented in Table

205   2 (cf. Equation II-A to II-F) (see Supplementary Data, Tables T7-T12 for the

206   corresponding ANOVA tables). In comparison with the complete model equations, in

207   most cases the values of R^2 decreased as the simplified fitted models exhibit lack-of-fit

208   and fail to predict $t_{50\%}$ for the experiments in which the effects of SBO and Fe(III)

209   concentrations on the response are important (see Supplementary Data, Figures F1-F6).

210   In other words, the effect of pH on the response is so pronounced that it masks the

211   effects of the other variables, especially that of SBO concentrations for some pH

212   conditions. For that reason, in order to discuss some trends concerning the effects of

213   SBO and Fe(III) concentrations and to better determine the pH domain where the photo-

214   Fenton could be applied, the complete fitted response surface models were considered,

215   and two-dimensional contour plots were built for each EP by fixing [SBO] at the higher

216   and lower values.

217

218   Figure 4A shows data obtained for carbamazepine. At low SBO concentration, a fast

219   decrease in the efficiency of photo-Fenton with increasing pH is observed, as the line

220   corresponding to $t_{50\%} = 20$ min can be found at a pH of ca. 4 and that of 60 min at a pH

221   of approximately 5.5. At low pH (below 4) an increase in [Fe(III)] results in a slight

222   enhancement of the process. This behaviour could be attributed to differences in iron

223   availability: at acidic medium, higher amounts of iron can be kept in solution, what

224   results in a faster degradation reaction; however, above pH = 4, SBOs are not able to

225   prevent efficiently iron precipitation and reaction rate decreases.

226

227 In contrast, at the highest SBO concentration (25 mg L^{-1}) a different trend can be found:

228 the loss of efficiency of the process occurs at higher pH, as differences are not acute in

229 the pH range 3-5.5, what suggests that SBOs are useful materials to apply the photo-

230 Fenton reaction at milder pH conditions. Furthermore, the optimum pH shifted to higher

231 values (ca. 4). This might indicate a change in the photo-Fenton mechanism, in which

232 the key species is not only Fe(OH)$^{2+}$ (responsible for the optimal pH value of 2.8), but

233 photoactive iron-SBO complexes might also contribute. Modification of the optimum

234 pH has already been described when species able to modify iron complexation are

235 present. For instance, at high concentration of chloride, photo-Fenton exhibits the best

236 performance at a pH slightly above 3 [21]. In addition, changes in photo-Fenton

237 mechanism at circumneutral values and or in the presence of chelating agent, such as

238 EDTA [22, 23] or citrate [24, 25], have been proposed, eventually changing the key

239 species [26]. Interestingly, when ethylenediamine-N,N'-disuccinic acid (EDDS) was

240 used as complexing agent, best results were reached at neutral or even slightly basic

241 medium; this variation was attributed to a completely different mechanism in which

242 superoxide plays a key role [27]. In the case of SBOs, experiments carried out with

243 chemical probes have shown that other species, in addition to •OH radicals, are

244 responsible for pollutants degradation [8-9].

245

246 Results obtained with clofibric acid (Figure 4E) and caffeine (Figure 4F) are very

247 similar to carbamazepine and for these compounds the photo-Fenton reaction showed to

248 be efficient until pH slightly above 5 at [SBO] of 25 mg L^{-1}. In fact, previous

249 experiments involving mild photo-Fenton conditions with non-complexed iron or in the

250 presence of humic substances or SBOs have demonstrated that they follow similar

251 behaviour with only quantitative differences. Acetamiprid (Figure 4D) is the most

252 recalcitrant compound towards the photo-Fenton process [8, 9]. This low reactivity

253 results in a poor efficiency of photo-Fenton, which quickly decreases with increasing

254 pH (the line of $t_{50\%}$ = 60 is at pH ca. 5 at low and high SBO concentrations).

255 Amoxicillin, on the other hand, is the most reactive among the EPs towards photo-

256 Fenton and at [SBO] = 25 mg L^{-1} shows the highest efficiency at pH = 5 and reaction

257 rate did not decrease significantly until values close to 7 (Figure 4C). Finally, for

258 acetominophen (Figure 4B) a slow but continuous decrease in reaction rate with

259 increasing pH is observed (line $t_{50\%}$ = 60 min at pH = 6). In fact, in a previous study [9]

260 this compound has been shown to have a different reactivity in comparison to the other

261 EPs, in which other species than $\bullet$OH play an important role.

262

263 Based on those results, it could be hypothesised that the presence of SBOs modifies the

264 photo-Fenton mechanism and, although some differences in the individual behaviour of

265 each EP have been evidenced, the process can be extended, in most cases, at least up to

266 pH = 5. Hence it is interesting to determine at this pH value the role of [Fe(III)] and

267 [SBO] in view of optimizing these variables. Contour plots obtained at pH = 5 for all six

268 EPs can be observed in Figure 5; the corresponding fitted equations are shown in Table

269 2 (cf. Table 2, Equations III-A to III-F) (see Supplementary Data for the ANOVA

270 tables, Tables T13-T18). In general, an optimum can be found in the region 4-5 mg L^{-1}

271 of iron and 19-22 mg L^{-1} of SBO, which should be considered as the best conditions for

272 the removal of the EPs from water by the photo-Fenton process. Under those conditions,

273 $t_{50\%}$ was ca. 20 min for all EPs, except for amoxicillin ($t_{50\%}$ < 10 min) and for

274 acetamiprid, which was the most refractory; in fact, acetamiprid was the only compound

275 which did not show a minimum for $t_{50\%}$ in the studied region.

276

277   The behaviour of SBO can be explained by considering that this species is necessary to

278   keep iron in solution and to allow the photo-Fenton process at pH = 5. However, beyond

279   a given point the role of SBO might be detrimental because it can act as scavenger of

280   the reactive species, competing with the pollutants, or because of a light screening effect

281   related to its brown colour. In the case of iron, it seems that amounts above 4 mg L^{-1}

282   play a negative role; this can be attributed to the faster precipitation of iron to form

283   oxides/hydroxides, which, in turn, decrease the photo-Fenton efficiency.

284

285   **Conclusions**

286

287   SBOs have been demonstrated as useful materials to allow the implementation of the

288   photo-Fenton processes at higher pH values (at least 5). This can be due to the ability of

289   these materials to complex iron, thus avoiding its precipitation as oxides or hydroxides.

290   The surface response methodology enabled to study the effect of iron, SBO and pH on

291   the process. Surface responses obtained at pH = 5 showed that optimal conditions of

292   Fe(III) and SBO concentrations were in the range   4-5 mg L^{-1} and 19-22 mg L^{-1}

293   respectively. Extending this methodology to other variables (e.g. H_2O_2 concentration) or

294   other compounds is a logical step forward.

295

296   Although a mechanistic study for such a complex system falls beyond the aim of this

297   study, our results seem to point to a modification of the photo-Fenton mechanism in

298   which the optimum pH shifts to higher values (in most cases in the range 3-4, slightly

299   above the optimal value described for photo-Fenton, 2.8). Furthermore, some

300   differences in the behaviour of each EP have been identified, which may be explained

301   by their reactivity with the new species formed, whose nature remains to be elucidated.

302   Hence, further research on the mechanistic issues of the process seems meaningful.

303

304   Finally, future work is also required to study the process at pH = 5 under real sunlight at

305   pilot plant with more realistic aqueous matrixes, estimating values such as H_2O_2

306   consumption, irradiation time or changes in biocompatibility, in order to better assess

307   the real applicability of this methodology.

308

314

315   **References**

316   [1] R.A.D. Arancon, C.S.K. Lin, K.M. Chan, T.H.Kwan, R. Luque, Energy Sci.

317   Technol, 1 (2013) 53-71.

318   [2] E. Montoneri, D. Mainero, V. Boffa, D.G. Perrone, C Montoneri, Int J. Global

319   Environ. Issues 11 (2011) 170-196.

320   [3] S. K. Khetan, T.J. Collins, Chem. Rev. 107 (2007) 2319-2364.

321   [4] A. Bianco Prevot, P. Avetta, D. Fabbri, E. Laurenti, T. Marchis, D.G. Perrone, E.

322   Montoneri, V. Boffa, ChemSusChem 4 (2011) 85-90.

323   [5] P. Avetta, F. Bella, A. Bianco Prevot, E. Laurenti, E. Montoneri, A. Arques, L.

324   Carlos, Sustainable Chem. Eng. 1 (2013) 1545-1550.

325   [6] P. Avetta, A. Bianco Prevot, D. Fabbri, E. Montoneri, L. Tomasso, L. Chem. Eng. J.

326   197 (2012) 193-198.

327   [7] A. Bianco Prevot, D. Fabbri, E. Pramauro, C. Baiocchi, C. Medana, E. Montoneri,

328   V. Boffa, J. Photochem. Photobiol. A: Chem. 209 (2010) 224-231.

329   [8] J. Gomis, R.F. Vercher, A.M. Amat, D.O. Martire, M.C. González, A. Bianco-

330   Prevot, E. Montoneri, A. Arques, L. Carlos. Catal. Today, 209 (2013) 176-180.

331   [9] J. Gomis, A. Bianco Prevot , E. Montoneri, M.C. González, A.M. Amat, D.O.

332   Mártire, A. Arques, L. Carlos, Chem. Eng. J. 235 (2014) 236-243.

333   [10] J.J. Pignatello, E. Oliveros, A. MacKay, Critical Rev. Environ. Sci. Technol. 36

334   (2006) 1-84.

335   [11] I. Carra, J.L. Casas López, L. Santos-Juanes, S. Malato, J.A. Sánchez Pérez, Chem

336   Eng. J. 224 (2013) 67-74.

337   [12] N. De la Cruz, L. Esquius, D. Grandjean, A. Magnet, A. Tungler, L.F. de

338   Alencastro, C. Pulgarin. Water Res. 47 (2013) 5836-5845.

339   [13] N. Klamerth, S. Malato, A. Agüera, A. Fernández-Alba. Water Res. 47 (2013) 833-

340   840.

341   [14] N. Klamerth, S. Malato, M.I. Maldonado, A. Agüera, A. Fernández-Alba, Catal.

342   Today 161 (2011) 241-246.

343 [15] A. Bernabeu, R.F.Vercher, L.Santos-Juanes, P.J.Simón, C.Lardín, M.A.Martínez,

344 J.A. Vicente, R.González, C.Llosá, A.Arques, A.M. Amat, Catal. Today, 161 (2011)

345 235-240.

346 [16] A. Bernabeu, S. Palacios, R.Vicente, R. Vercher, S.Malato, A. Arques, A.M.

347 Amat. Chem Eng. J. 198-199 (2012) 65-72.

348 [17] D.H. Doehlert. Uniform shell designs. J R Stat Soc.,Ser C 19 (1970) 231–239.

349 [18] M.A. Bezerra, R.E. Santelli, E.P. Oliveira, L.S.Villar, L.A. Escaleira, Talanta 76

350 (2008) 965–977.

351 [19] E. Montoneri, D. Mainero, V. Boffa, D.G. Perrone, C. Montoneri, Int. J. Global

352 Environ. Issues 11 (2011) 170-196.

353 [20] S. L. C. Ferreira, W. N. L. dos Santos, C. M. Quintella, B. B. Neto, J. M. Bosque-

354 Sendra, Talanta 63 (2004) 1061-1067.

355 [21] A. Machulek, J.E.F. Moraes, C. Vautier-Giongo, C.A. Silverio, L.C. Friedrich,

356 C.A.O. Nascimento, M.C. González, F Quina, Environ. Sci. Technol. 41 (2007) 8459–

357 8463.

358 [22] N. Klamerth, S. Malato, A. Agüera, A. Fernández-Alba, G. Mailhot, Environ. Sci.

359 Technol. 46 (2012) 2885-2892.

360 [23] J.D. Rush, W.H. Koppenol, J. Biol. Chem. 261 (1986), 6730-6733.

361 [24] M.R.A. Silva, A.G. Trovó, R.F.P. Nogueira, J. Photochem. Photobiol A: Chem.

362 191 (2007) 187-192

363 [25] H. Katsumata, S. Kaneco, T. Suziki, K. Ohta, Y. Yobiko, J. Photochem. Photobiol

364 A: Chem.180 (2006) 38-45.

365   [26] S.J. Hug, O. Leupin, Environ. Sci. Technol. 37 (2003), 2734-2742.

366   [27] W. Huang, M. Brigante, F. Wu, C. Mousty, K. Hanna, G. Mailhot, Environ. Sci.

367   Technol. 47 (2013) 1952-1959

368

Exp number	[Fe(III)]	[SBO]	pH	A	B	C	D	E	F
1	4	20	5	21.6	25.8	14.4	57.6	24.3	25.5
1'	4	20	5	18.1	24.9	16	54.1	24.6	26.6
1''	4	20	5	15	22	10	48.8	20.4	23.2
2	6	20	5	23.8	26.6	12.8	59.5	28.2	31.3
3	5	25	5	27.8	33.8	22	68.9	32.1	36.4
4	2	20	5	27.9	28.4	24.4	57	29.5	35.1
5	3	15	5	34.4	41.6	26.3	83.9	40.3	47.1
6	5	15	5	33.3	36.4	24.4	68.9	36.1	39.6
7	3	25	5	27.5	33	22.3	65.8	33.7	35.8
8	5	21.7	7	129.4	86.3	111.5	320	133.3	207.5
9	3	21.7	7	88.4	82.1	62.4	218	87.4	109.7
10	4	16.7	7	154	75.5	174.3	242.7	156.4	150
11	3	18.3	3	2.3	3.3	2.3	6.4	2.7	3.1
12	5	18.3	3	1.7	1.5	1	3.9	2.1	1.8
13	4	23.3	3	1.3	2.4	1.3	4.6	1.8	2.1

369

370 Table 1: Experimental points used to obtain the response surface (Doehlert matrix). The

371 concentrations of SBO and iron are expressed as mg L^{-1}; data given in the last six

372 columns correspond to the time (in min) required to decrease concentration of each EP

373 to 50% of the initial value for carbamazepine (A), acetaminophen (B), amoxicillin (C),

374 acetamiprid (D), clofibric acid (E) and caffeine (F)

375

Compound	Equation
Carbamazepine	$t_{50\%}$ (min) = 248.38 − 40.37·[Fe] − 8.52·[SBO] − 51.39·pH + 1.90·[Fe]^2 + 0.07 [Fe][SBO] + 5.14·[Fe]·pH + 0.43 [SBO]^2 − 2.08·[SBO]·pH + 10.28·pH^2 (R^2 = 0.974) (I-A) $t_{50\%}$ (min) = 106.29 − 62.86 pH + 9.34 pH^2 (R^2 = 0.915) (II-A) $t_{50\%}$ (min) = 239.50 − 17.38·[Fe] − 17.88 [SBO] + 1.90 [Fe]^2 + 0.43 [SBO]^2 + 0.07 [Fe][SBO] (R^2 = 0.930) (III-A)
Acetominophen	$t_{50\%}$ (min) = 318.33 − 15.36·[Fe] − 22.79·[SBO] − 32.82·pH + 0.82·[Fe]^2 + 0.30 [Fe][SBO] + 0.50 [Fe] pH + 0.45 [SBO]^2 + 0.71·[SBO]·pH + 3.64·pH^2 (R^2 = 0.994) (I-B) $t_{50\%}$ (min) = 3.98 − 9.21 pH + 2.89 pH^2 (R^2 = 0.963) (II-B) $t_{50\%}$ (min) = 253.57 − 13.20·[Fe] − 19.60 [SBO] + 0.82 [Fe]^2 + 0.45 [SBO]^2 + 0.3 [Fe][SBO] (R^2 = 0.972) (III-B)
Amoxicillin	$t_{50\%}$ (min) = 56.92 − 41.63·[Fe] + 3.80·[SBO] − 19.34·pH + 1.28·[Fe]^2 + 0.08 [Fe][SBO] + 6.23·[Fe]·pH + 0.36 [SBO]^2 − 4.19·[SBO]·pH + 10.69·pH^2 (R^2 = 0.924) (I-C) $t_{50\%}$ (min) = 123.65 − 70.42 pH + 9.91 pH^2 (R^2 = 0.794) (II-C) $t_{50\%}$ (min) = 199.27 − 13.98·[Fe] − 15.04 [SBO] + 1.28 [Fe]^2 + 0.36 [SBO]^2 + 0.08 [Fe][SBO] (R^2 = 0.879) (III-C)
Acetamiprid	$t_{50\%}$ (min) = 966.42 − 83.28·[Fe] − 40.02·[SBO] − 206.76·pH + 1.19·[Fe]^2 + 0.91·[Fe]·[SBO] + 12.29·[Fe]·pH+ 0.69·[SBO]^2 + 1.77·[SBO]·pH + 18.59·pH^2 (R^2 = 0.981) (I-D) $t_{50\%}$ (min) = 180.38 − 110.88 pH + 17.47 pH^2 (R^2 = 0.946) (II-D) $t_{50\%}$ (min) = 440.30 − 28.18·[Fe] − 32.03 [SBO] + 1.19 [Fe]^2 + 0.69 [SBO]^2 + 0.91 [Fe][SBO] (R^2 = 0.915) (III-D)
Clofibric acid	$t_{50\%}$ (min) = 242.78 − 40.30·[Fe] − 9.39·[SBO] − 44.58·pH + 1.44·[Fe]^2 + 0.13 [Fe][SBO] + 5.70·[Fe]·pH + 0.44 [SBO]^2 − 2.06·[SBO]·pH + 9.40·pH^2 (R^2 = 0.971) (I-E) $t_{50\%}$ (min) = 88.28 − 54.22 pH + 8.51 pH^2 (R^2 = 0.907) (II-E) $t_{50\%}$ (min) = 246.10 − 14.80·[Fe] − 18.67 [SBO] + 1.44 [Fe]^2 + 0.44 [SBO]^2 + 0.13 [Fe][SBO] (R^2 = 0.955) (III-E)
Caffeine	$t_{50\%}$ (min) = 702.53 − 79.39·[Fe] − 25.36·[SBO] − 147.13·pH + 2.02·[Fe]^2 + 0.41 [Fe][SBO] + 12.04·[Fe]·pH + 0.50·[SBO]^2 + 0.65 [SBO] pH + 12.44·pH^2 (R^2 = 0.959) (I-F) $t_{50\%}$ (min) = 126.86 − 75.73 pH + 11.41 pH^2 (R^2 = 0.890) (II-F) $t_{50\%}$ (min) = 310.83 − 25.51·[Fe] − 22.51 [SBO] + 2.03 [Fe]^2 + 0.50 [SBO]^2 + 0.41 [Fe][SBO] (R^2 = 0.984) (III-F)

376

377 Table 2: Response surface models obtained for each EP, where the values of the

378 variables are specified in their original units. (I) refer to the complete fitted model, (II)

379 to the simplified fitted model without the non-significant variables, and (III) to the fitted

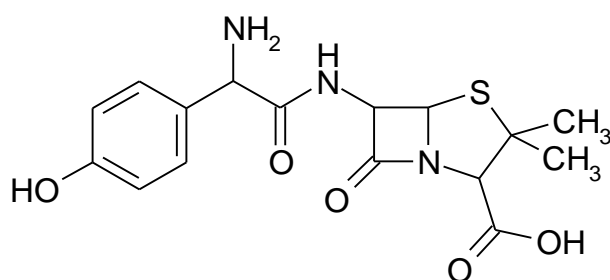380 model considering only the experiments performed at pH 5

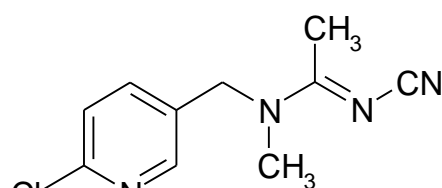Figure 1: Chemical structures of EPs used in this study
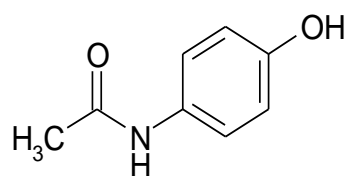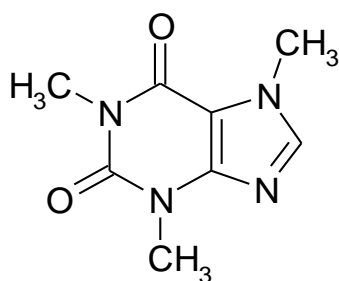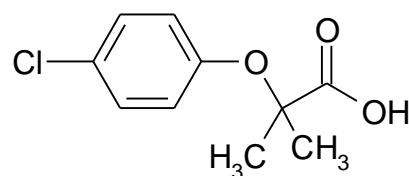
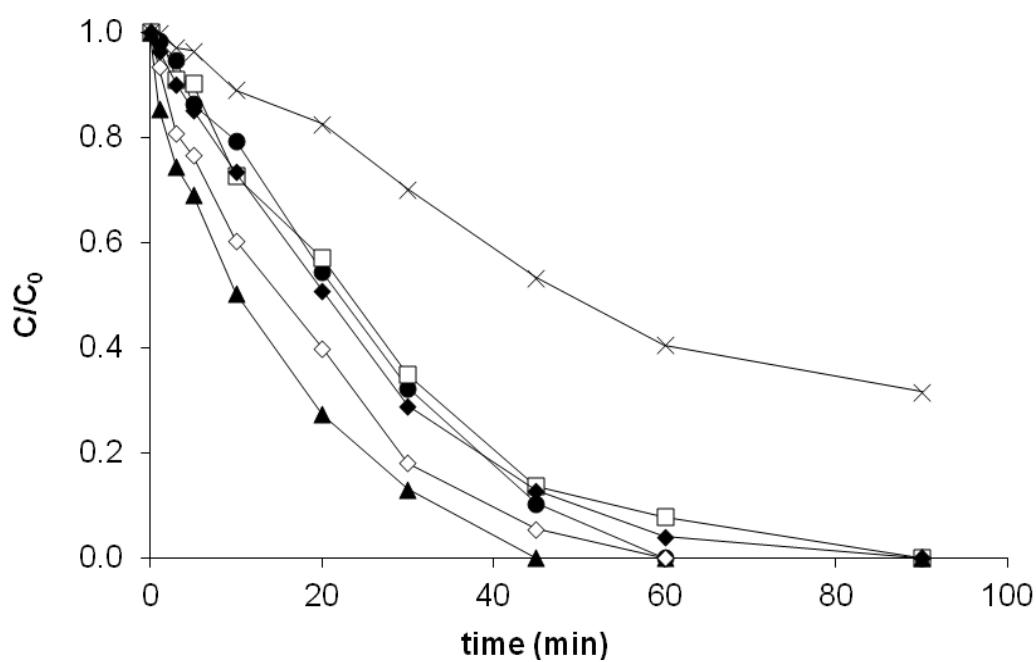Acetominophen
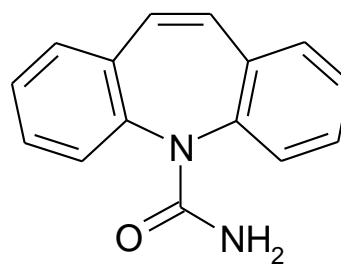
Carbamazepine

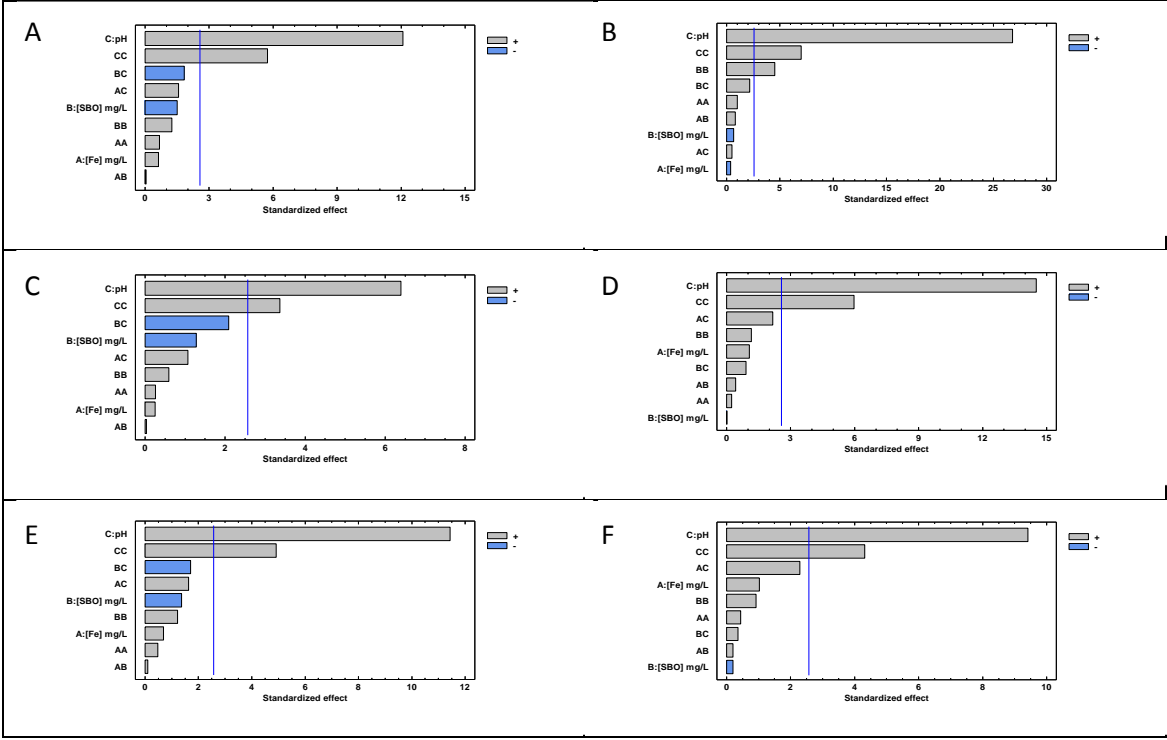Amoxicillin

Acetamiprid

Caffeine

Clofibric acid

382 Figure 2: Example of the photodegradation of a mixture of 6 EPs by means of the
383 photo-Fenton reaction. Plot of the relative concentration vs time: amoxicillin (▲),
384 acetaminophen (●), acetamiprid (×), caffeine (□), clofibric acid (♦) and carbamazepine
385 (◊). Data correspond to the central point ([SBO] = 20 mg L^{-1}, [Fe(III)] = 4 mg L^{-1}, pH =
386 5)

387

388

389

390 Figure 3: Pareto charts for the response $t_{50\%}$ (min) obtained for the photo-Fenton

391 degradation of EPs in the presence of SBO. The EPs are carbamazepine (A),

392 acetaminophen (B), amoxicillin (C), acetamiprid (D), clofibric acid (E) and caffeine (F)
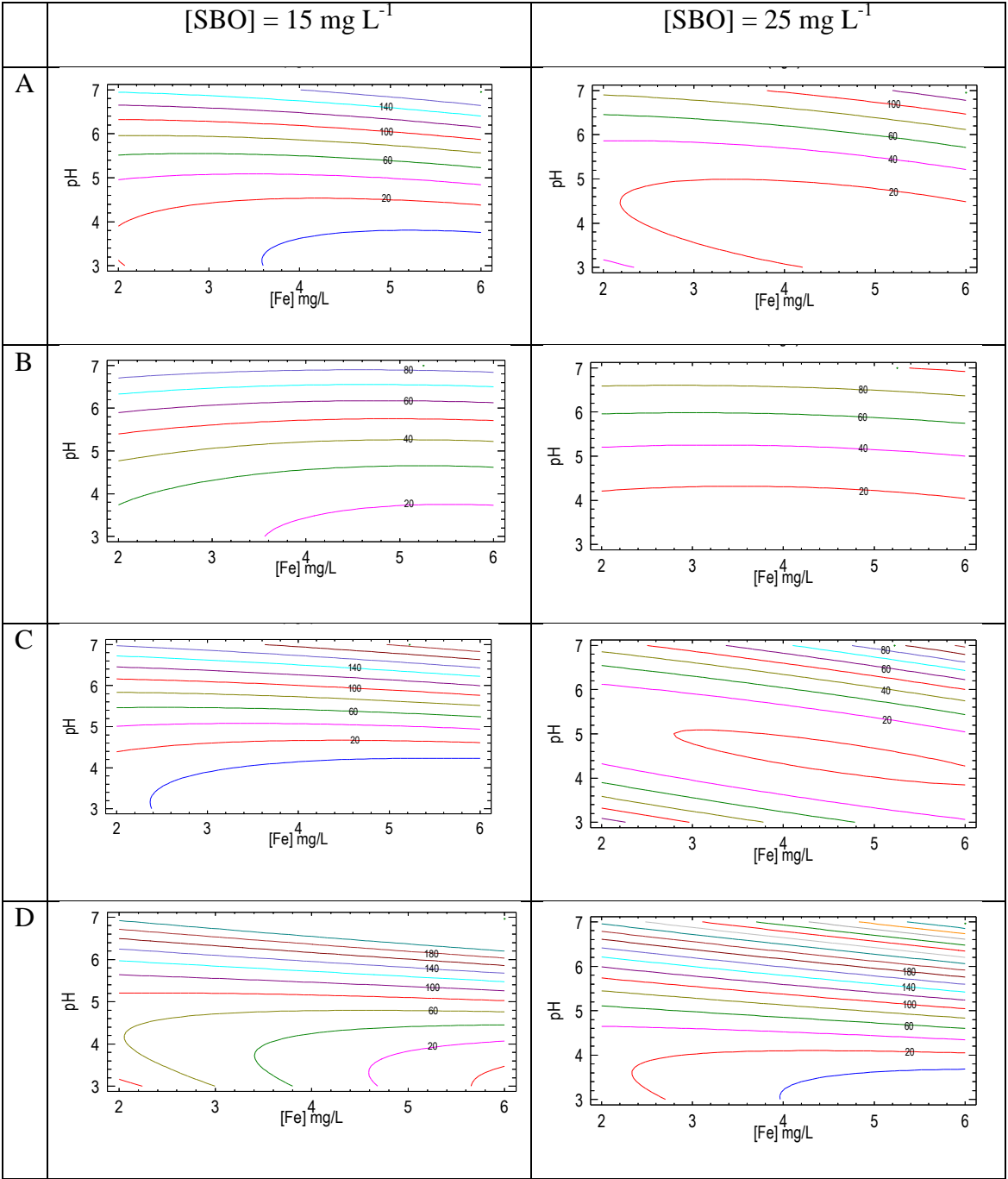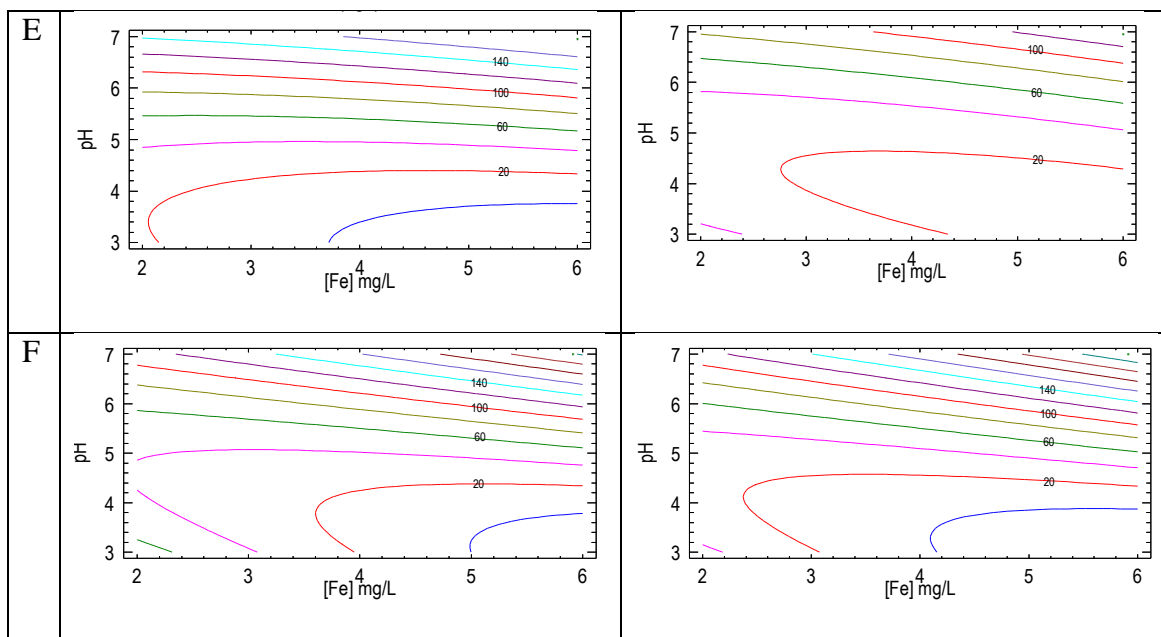

393

394

395 Figure 4: Contour plots for $t_{50\%}$ (min) obtained for the photo-Fenton degradation of EPs

396 in the presence of SBO. The EPs are carbamazepine (A), acetaminophen (B),

397 amoxicillin (C), acetamiprid (D), clofibric acid (E) and caffeine (F)

398

Figure 5: Contour plots for $t_{50\%}$ (min) obtained for the photo-Fenton degradation of EPs

404 at pH = 5. The EPs are carbamazepine (A), acetaminophen (B), amoxicillin (C),

405 acetamiprid (D), clofibric acid (E) and caffeine (F)

406